Michael Klum*, Mike Urban, Alexandru-Gabriel Pielmus and Reinhold Orglmeister

# Dual-Lead 55 mm Impedance Pneumography

**Abstract:** In recent years, respiratory monitoring has gained attention due to the high prevalence and severe consequences of sleep apnea, post-anesthesia respiratory instability and respiratory diseases. Nevertheless, respiratory monitoring oftentimes relies on obtrusive masks and belts, which are unsuitable for wearable, long-term monitoring. Impedance pneumography (IP) is a bioimpedance method aiming to assess respiratory parameters unobtrusively. However, most IP configurations require far-spaced electrodes. Based on our recent work on wearable IP, we propose a dual-lead, wearable IP setup with 55 mm electrode spacing to estimate respiratory flow and rate (RR). Using our recently presented multimodal patch stethoscope as well as commercial systems, we conducted a study including 10 healthy subjects which were recorded in the supine, lateral and prone position. Using time-delay neural networks, we achieved RR estimation errors below 0.6 breaths per minute and flow correlations of 0.88 with relative errors of 25 % to a pneumotachometer reference. We conclude that dual-lead IP increases the performance of respiratory signal estimation compared to a single lead and recommend research in the area of subject position dependency and movement artefacts.

**Keywords:** multi-lead bioimpedance, wearable impedance pneumography, wearable respiratory monitoring, respiratory rate, respiratory flow, sensor patch, neural network

https://doi.org/10.1515/cdbme-2020-3052

## 1 Introduction

Respiratory monitoring gains importance in the context of the highly prevalent [1] and consequential [2] obstructive sleep apnea, effecting an estimated 936 million people worldwide. Respiratory instability is also known to worsen the clinical outcome [3] and the current COVID-19 pandemic further emphasizes the need for respiratory diagnostics [4]. Nevertheless, most respiratory monitors rely on obtrusive sensors including belts or nasal cannula pressure sensors. A promising development towards unobtrusive respiratory monitoring is impedance pneumography (IP), a method in the family of bioimpedance applications [5]. Oftentimes, ECG electrodes are used to simultaneously acquire IP. This leads to long inter-electrode distances, which is beneficial for IP performance but hinders its unobtrusive implementation. Currently, optimization of electrode positions mainly aims to increase linearity with respect to lung volume [6]. Jeyhani et al., however, proposed a short distance configuration spanning the half thorax [7]. Our workgroup presented a 55 mm wearable IP concept [8] using our novel, multimodal patch stethoscope [9], raising the question if flow estimation can be improved when using multiple wearables. Cohen et al. first analyzed multiple IP leads using regression [10]. Gracia et al. presented a multi-lead impedance measurement system [11], later used to assess lung tissue mechanics. Most recently, Sel et al. [12] used a total of four devices in conjunction with blind source separation to extract respiration rate (RR) and heart rate from impedance signals.

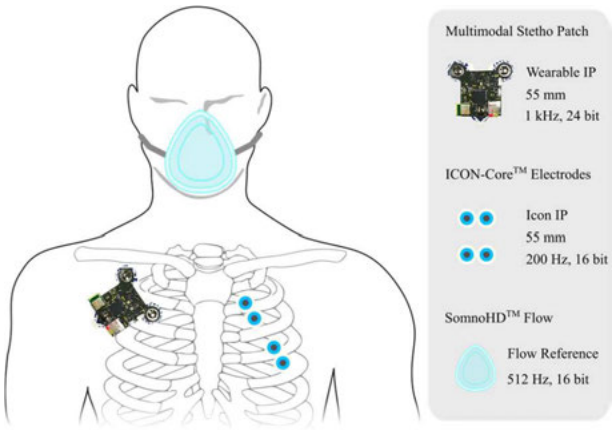


**Figure 1:** Study setup for 55 mm wearable and Icon IP.

Building on the promising results of our wearable IP concept, we demonstrate the use of two independent 55 mm IP leads to estimate respiratory flow and rate with data from both lungs from 10 healthy subjects using time-delay neural network regression models. In a nested cross-validated, model selection framework, respiratory signals were estimated in the supine, lateral and prone position.

***Corresponding author: Michael Klum:** Chair of Electronics and Medical Signal Processing, Technische Universität Berlin, Einsteinufer 17, 10587 Berlin, Germany,
e-mail: michael.klum@tu-berlin.de
**Mike Urban, Alexandru-Gabriel Pielmus, Reinhold Orglmeister:** Chair of Electronics and Medical Signal Processing, Technische Universität Berlin, Einsteinufer 17, Berlin

# 2 Materials and Methods

## 2.1 Data Acquisition

In a study including 10 healthy subjects (26±2 years, 2 female), participants lay in the supine, lateral and prone position while following a breathing protocol displayed by a tablet running a custom developed Android application. The 11-minute long sequence contained three breathing frequencies (8, 16 and 24 breaths per minute (bpm)) and two breathing depths (shallow, normal), resulting in 33 minutes of data per participant and more than 5 hours in total.

Two 55 mm IP leads were simultaneously recorded alongside a respiratory reference (512 Hz, 16 bit), provided by the SOMNOmedics GmbH SOMNO HD™ using a pneumotachometer and facial mask. The 55 mm wearable IP signal (1 kHz, 24 bit) was acquired between the first and second intercostal spaces (ICS) at the right midclavicular line at an angle of 45 ° using the stethoscope patch. The 55 mm Icon IP (200 Hz, 16 bit) was recorded by the Osypka Medical GmbH ICON-Core™ monitor between the 2nd and 3rd ICS centered on the left midclavicular line at an angle of 45 °. The positions, given in Figure 1, are a compromise between robust placement, comfort and lung coverage. Crosstalk was avoided by using different measurement frequencies.

## 2.2 Signal Processing and Regression

The IP, as well as respiratory flow signals, have been band-limited between 0.05 Hz and 1 Hz using baseline removal and low pass filtering. The first derivatives of the IP signals were used for a flow surrogate, as it represents the change of the estimated volume. Flow and RR estimation performances of both IP configurations were first assessed individually. We then simulated the simultaneous application of two wearable IP systems by using both IP signals as independent variables in a combined regression. RR has been estimated using the maximum of the FFT between 4 and 40 bpm in 30 s windows with a 50 % overlap in all cases.

Time-delay neural networks (TDNN) consistently outperformed polynomials and multilayer perceptrons in our previous study [8]. Therefore, only TDNN-based regression was employed. We analyzed configurations of 2 to 3 hidden layers with 2 to 15 neurons each and input delay vector lengths of 1 to 30 taps. Model selection was performed using the Bayesian information criterion (BIC). The mean error (ME), mean absolute error (MAE) and Pearson correlation (r) were used to assess the performances of both the respiratory flow and rate estimates $Est$ relative to the references $Ref$.

For strictly non-zero data, here the RR, we used the mean absolute percentage error (MAPE) calculated as

$$MAPE = \frac{1}{N}\sum_{i=1}^{N}\left|\frac{Est(i) - Ref(i)}{Ref(i)}\right| * 100\ \%. \qquad (1)$$

For data including or closely approaching zero, in the presented study the respiratory flow, the MAPE can become singular. Therefore, we employed the normalized mean squared error (NMSE) in this case, given as

$$NMSE = \frac{\sum_{i=1}^{N}(Est(i) - Ref(i))^2}{\sum_{i=1}^{N} Ref(i)^2} * 100\ \%. \qquad (2)$$

The performances were assessed individually and for each position using nested cross-validation in a forward-chaining training, validation and test data splitting scheme.

# 3 Results

During the model selection, TDNNs with two hidden layers, 6 neurons each and delay input line lengths of 14 taps were chosen based on the BIC. For the subsequent analysis, performances shown are based on this configuration. In Table 1, the performances of the respiratory flow estimation using Icon IP, wearable IP, and dual-lead IP regression are given.

**Table 1:** Performance of respiratory flow estimations per subject position and IP configuration using TDNN regression.

| Pose | Config | $ME_{ml/s}$ | $MAE_{ml/s}$ | r | $NMSE_{\%}$ |
|---|---|---|---|---|---|
| Supine | Icon | -9.8±16.1 | 138.9±96.8 | 0.73±0.25 | 43±32 |
| | Wearable | 0.7±9.2 | 114.2±46.6 | 0.87±0.04 | 30±9 |
| | Dual-Lead | -2.3±17.1 | 102.8±50.3 | 0.89±0.05 | 25±9 |
| Lateral | Icon | 3.3±13.3 | 116.5±51.8 | 0.83±0.17 | 34±25 |
| | Wearable | -2.6±10.4 | 123.6±61.1 | 0.84±0.10 | 33±18 |
| | Dual-Lead | -4.4±10.9 | 100.4±43.1 | 0.91±0.04 | 23±10 |
| Prone | Icon | -2.1±11.8 | 103.5±65.6 | 0.85±0.19 | 26±25 |
| | Wearable | 2.8±17.8 | 161.6±50.6 | 0.68±0.18 | 53±22 |
| | Dual-Lead | -2.4±6.2 | 98.6±54.1 | 0.87±0.16 | 23±20 |
| **All** | Icon | -4.0±12.0 | 120.6±72.2 | 0.81±0.19 | 36±28 |
| | Wearable | 4.9±12.6 | 133.3±51.3 | 0.80±0.13 | 40±18 |
| | **Dual-Lead** | **-1.3±11.3** | **100.8±47.0** | **0.88±0.10** | **25±14** |

Exemplary signals of the flow reference as well as the three regression model estimates are shown in Figure 2. Both the wearable and Icon IP curves show over- and underestimations of the flow between 100 ml/s and 200 ml/s with a low bias, which is in accordance with the average performances reported. The dual-lead IP regression model shows an overall better tracking of the reference flow curve. Specifically, in the presence of a change of the peak flow rate, visible in the signal at 10 s, the dual-lead regression provides an overall more consistent approximation.

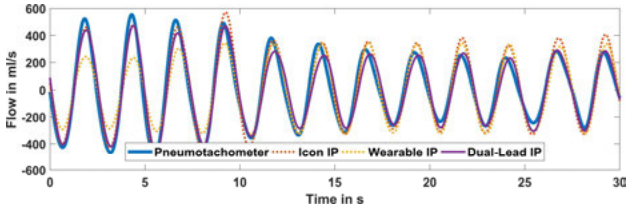


**Figure 2:** Exemplary reference and estimated respiratory signals.

Table 2 gives the results of the RR estimation for each position and the three IP regression configurations including outliers. In both the wearable and Icon IP configurations, 15% of the data have been identified as outliers, defined as points more than three scaled median absolute deviations away from the median. In the dual-lead IP approach, 8 % outliers have been found. When removed, the dual-lead IP RR estimation achieves an ME of -0.012 bpm, an MAE of 0.085 bpm, a correlation of 0.98 and a MAPE of 0.72 %.

**Table 2:** Performances of the respiratory rate estimation including outliers per subject position using found optimal TDNNs.

| Pose | Config | $ME_{bpm}$ | $MAE_{bpm}$ | r | $MAPE_{\%}$ |
|---|---|---|---|---|---|
| | Icon | 0.1±3.7 | 1.2±3.5 | 0.89±0.14 | 9±30 |
| Supine | Wearable | 0.4±3.9 | 1.2±3.8 | 0.88±0.21 | 11±43 |
| | Dual-Lead | 0.1±2.2 | 0.5±2.1 | 0.96±0.07 | 4±20 |
| | Icon | 0.2±1.9 | 0.6±1.8 | 0.97±0.05 | 5±20 |
| Lateral | Wearable | 0.5±4.3 | 1.4±4.1 | 0.86±0.17 | 14±45 |
| | Dual-Lead | -0.4±2.4 | 0.5±2.4 | 0.95±0.08 | 3±11 |
| | Icon | 0.3±2.4 | 0.5±2.4 | 0.97±0.09 | 3±14 |
| Prone | Wearable | 0.3±4.2 | 1.4±3.9 | 0.86±0.13 | 13±40 |
| | Dual-Lead | -0.0±0.2 | 0.1±0.2 | 1.00±0.00 | 1±2 |
| | Icon | 0.4±3.3 | 0.9±3.2 | 0.92±0.16 | 8±30 |
| **All** | Wearable | 0.5±4.3 | 1.4±4.1 | 0.87±0.17 | 14±47 |
| | **Dual-Lead** | **-0.0±2.5** | **0.5±2.4** | **0.95±0.12** | **4±24** |

Figure 3 visualizes the RR estimation performance using a Bland-Altman plot. The three breathing rate clusters correspond to the three distinct frequencies in the study setup. Their compact appearance further proposes a narrow error distribution that is contaminated by large and implausible outliers. A rate-dependent error distribution or a systematic error was not found.

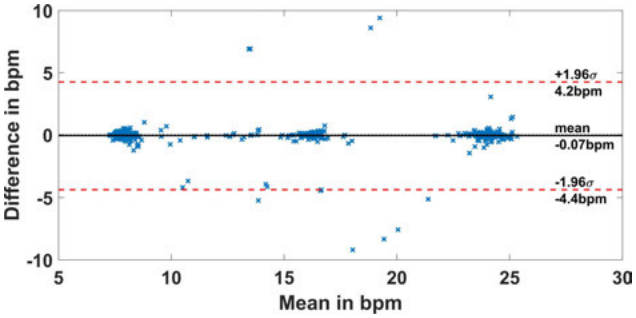


**Figure 3:** Bland-Altman plot of the dual-lead IP respiratory rate estimation performance including all subject positions.

# 4 Discussion

The average performances of the 55 mm wearable IP and the 55 mm Icon IP reported here are consistent with our findings for wearable IP flow (r: 0.81, NMSE: 38%) and RR estimation (r: 0.9, MAPE: 8%) [8]. With two studies and two measurement systems agreeing closely, the applicability of wearable IP is further supported. In the wearable IP setup, performances vary with subject positions consistently with [8], the supine position being the most and the prone position the least optimal. The Icon IP, however, showed an opposing trend. We suspect that the tetra-polar measurement scheme of the Icon IP is more stable than the bipolar setup of the wearable IP. In addition, the Icon IP electrodes are placed slightly lower than the wearable setup and the injecting electrodes are spaced further apart. A definite conclusion on which position is most vulnerable to errors cannot be drawn based on the data presented here, due to inconsistencies between the performances of the different lead systems. Further research in the area of position dependency and movement artifacts is recommended.

The dual-lead IP regression did increase the flow estimation performance compared to the single, wearable IP leads. The linear correlation increased from 0.80 and 0.81 respectively to 0.88 over all positions and subjects. The relative error was reduced from 36 % and 40 % to 25 %. In addition, standard deviations were reduced in most cases. The previous assumption that, covering the two lungs with

separate, minimal IP systems increases performance can, therefore, be confirmed. When compared to the performance of the half-thorax configuration (r: 0.94, NMSE: 16%) [8], the dual-lead 55 mm IP approach is less optimal. We assume that the volume in the lower lung lobes on both sides is not captured by the dual-lead IP systems and therefore mainly contributes to the error. The dependency of the estimation errors on the subject position was minimal

The RR estimation correlation increased in the dual-lead IP application from 0.92 and 0.87 to 0.95 and the MAPE was reduced from 8 % and 14 % to 4 %. Compared to the half-thorax performance (r: 0.97, MAPE: 2 %) [8], the performance of the dual-lead IP is comparable, showing the reduced importance of accurate flow curve tracking for RR estimation performances. Removing outliers, the same performance values as reported for the half-thorax configuration have been obtained. The subject position dependency of the estimation errors was minimal.

The main limitation of the presented work is the number of subjects included in the study which, in addition, were mostly young, healthy and male. This limitation, however, is attenuated by the comparison with previous studies.

# 5 Summary and Conclusion

We presented a 55 mm dual-lead impedance pneumography (IP) setup covering both lung lobes to estimate respiratory flow and rate in the supine, lateral and prone position. Using both IP signals in a time-delay neural network regression model, we estimated the flow with a correlation of 0.88 and a relative error of 25 % with respect to a pneumotachometer reference. Respiratory rate estimation errors were below 0.6 bpm in all cases. The subject dependency of the estimation errors was minimal.

We conclude that using two independent, wearable IP leads can substantially increase the respiratory flow and rate estimation performance compared to a single lead. Performances close to half-thorax configurations can be achieved. Further research could focus on subject position dependencies and the influence of motion on the signals.

### Author Statement

Research funding: The author state no funding involved. Conflict of interest: Mike Urban is currently employed at Osypka Medical GmbH. Informed consent: Informed consent has been obtained from all individuals included in this study. Ethical approval: The research is approved by the TU Berlin Ethics Committee of the Department of Psychology and Ergonomics under the tracking number KL_01_20180117.

## References

[1] A. V. Benjafield, et al., "Estimation of the global prevalence and burden of obstructive sleep apnoea: a literature-based analysis," The Lancet Respiratory Medicine, vol. 7, pp. 687-698, 2019.

[2] G. Cadby, et al., "Severity of OSA is an independent predictor of incident atrial fibrillation hospitalization in a large sleep-clinic cohort," Chest, vol. 148, pp. 945-952, 2015.

[3] A. Fernandez-Bustamante, et al., "Postoperative pulmonary complications, early mortality, and hospital stay following noncardiothoracic surgery: a multicenter study by the perioperative research network investigators," JAMA surgery, vol. 152, pp. 157-166, 2017.

[4] World Health Organization, "Coronavirus disease 2019 ( COVID-19): situation report, 51," 2020.

[5] D. Naranjo-Hernández, et al., "Fundamentals, Recent Advances, and Future Challenges in Bioimpedance Devices for Healthcare Applications," Journal of Sensors, vol. 2019, pp. 1-42, 7 2019.

[6] V.-P. Seppä, et al., "Novel electrode configuration for highly linear impedance pneumography," Biomedizinische Technik/Biomedical Engineering, vol. 58, pp. 35-38, 2013.

[7] V. Jeyhani, et al., "Optimal Short Distance Electrode Locations for Impedance Pneumography Measurement from the Frontal Thoracic Area," XIV Mediterranean Conference on Medical and Biological Engineering and Computing 2016, pp. 1144-1149, 2016.

[8] M. Klum, et al., "Wearable Impedance Pneumography," Current Directions in Biomedical Engineering, 2020.

[9] M. Klum, et al., "Wearable Multimodal Stethoscope Patch for Wireless Biosignal Acquisition and Long-Term Auscultation," in 2019 41st Annual International Conference of the IEEE Engineering in Medicine and Biology Society (EMBC), 2019.

[10] C. J. Upton, et al., "Combined impedance and inductance for the detection of apnoea of prematurity," Early human development, vol. 24, pp. 55-63, 1990.

[11] J. Gracia, et al., "Multilead measurement system for the time-domain analysis of bioimpedance magnitude," IEEE transactions on biomedical engineering, vol. 59, pp. 2273-2280, 2012.

[12] K. Sel, et al., "Measurement of chest physiological signals using wirelessly coupled bio-impedance patches," in 2019 41st Annual International Conference of the IEEE Engineering in Medicine and Biology Society (EMBC), 2019.